◆ Human Brain Mapping 34:2607–2623 (2013) ◆

Neural Correlates of Visual Search in Patients With Hereditary Retinal Dystrophies

Tina Plank,[1]* Jozef Frolo,[1] Fatima Farzana,[1] Sabine Brandl-Rühle,[2] Agnes B. Renner,[2] and Mark W. Greenlee[1]

[1]*Institute of Psychology, University of Regensburg, Germany*
[2]*Department of Ophthalmology, University Medical Center Regensburg, Germany*

Abstract: In patients with central visual field scotomata a large part of visual cortex is not adequately stimulated. We investigated evidence for possible upregulation in cortical responses in 22 patients (8 females, 14 males; mean age 41.5 years, range 12–65 years) with central visual field loss due to hereditary retinal dystrophies (Stargardt's disease, other forms of hereditary macular dystrophies and cone-rod dystrophy) and compared their results to those of 22 age-matched controls (11 females, 11 males; mean age, 42.4 years, range, 13–70 years). Using functional magnetic resonance imaging (fMRI) we recorded differences in behavioral and BOLD signal distribution in retinotopic mapping and visual search tasks. Patients with an established preferred retinal locus (PRL) exhibited significantly higher activation in early visual cortex during the visual search task, especially on trials when the target stimuli fell in the vicinity of the PRL. Compared with those with less stable fixation, patients with stable eccentric fixation at the PRL exhibited greater performance levels and more brain activation. *Hum Brain Mapp 34:2607–2623, 2013.* © 2012 Wiley Periodicals, Inc.

Key words: hereditary retinal dystrophy; central visual field scotomata; visual cortex; functional magnetic resonance imaging, visual search task

INTRODUCTION

The cone photoreceptors in the macula are essential for high visual acuity. When macular function is compromised, patients complain about reduced visual acuity, reading difficulties, disturbed color vision and central scotoma in their visual field. One of the most common hereditary macular dystrophies is Stargardt's disease. It results in a progressive macular dysfunction with ongoing visual loss over months or years. Another generalized retinal dystrophy, the cone-rod dystrophy (CRD), starts in the macula and affects also the peripheral retina during disease progression. Patients with identical clinical features can exhibit different levels of visual impairment [Crossland et al., 2005]. Clinicians frequently ascribe these differences to adaptive strategies adopted by patients. One such adaptive strategy is to use the healthy eccentric parts of the retina for fixation. When an absolute scotoma prevents foveal fixation, the patient uses an eccentric location on the retina to fixate by directing their gaze away from the target. With time, most patients establish one specific eccentric retinal area as a kind of pseudo-fovea, called the "preferred retinal locus" [PRL; Bäckman and Inde, 1979; Fletcher and Schuchard, 1997; Guez et al., 1993; Timberlake et al., 1987; Whittaker et al., 1988]. Since the patients use this particular area in the peripheral visual field for everyday visual tasks, like reading or identification of objects and faces, the processing of visual input from this

Contract grant sponsor: Deutsche Forschungsgemeinschaft (Research Group FOR 1075: Regulation and Pathology of Homeostatic Processes in Visual Function).

*Correspondence to: Tina Plank, Institut für Psychologie, Universität Regensburg, Universitätsstr. 31, 93053 Regensburg, Germany. E-mail: tina.plank@psychologie.uni-regensburg.de

Received for publication 13 April 2011; Revised 13 February 2012; Accepted 7 March 2012

DOI: 10.1002/hbm.22088

Published online 16 April 2012 in Wiley Online Library (wileyonlinelibrary.com).

© 2012 Wiley Periodicals, Inc.

part of the visual field presumably undergoes extensive training over time. As is known from studies on perceptual learning, the visual system shows remarkable and long-lasting improvements when trained to perform demanding visual tasks and these changes have been attributed to neural plasticity on the sensory level of the adult brain [e.g., Ahissar and Hochstein, 1997; Fahle and Poggio, 2002; Gilbert et al., 2001; Karni and Sagi, 1991; Schoups et al., 1995; Watanabe et al., 2001]. Several studies have shown that such learning effects are specific to the trained location and/or stimulus feature, suggesting that early visual cortices exhibit neuroplasticity associated with learning [e.g., Furmanski et al., 2004; Schoups et al., 2001; Schwartz et al., 2002; Sigman et al., 2005; Yotsumoto et al., 2008]. In this study we investigate the neural representation of the PRL projection zone of patients with central scotomata. As an adjustment to the disease the PRL becomes a highly trained location in the visual field, used by the patients for tasks like reading, which are normally reserved to the fovea. We assume that perceptual learning has taken place in the peripheral visual field of those patients, especially at the PRL projection zone. This learning should be reflected in an enhanced activation of early visual cortex (areas V1–V3). In this study, we determined activation patterns in early visual areas using functional magnetic resonance imaging (fMRI), while participants performed a visual search task. In this task the participants had to detect the letter "L" (target stimulus) presented among several distractor-letters "T" which were arranged radially in the peripheral visual field. Thus the task contained the identification of well-trained shapes ("letters") at different positions in the eccentric visual field, including the patients' PRLs. We investigated 22 patients with central visual field loss due to hereditary retinal dystrophies and compared their results to those of 22 age-matched controls. Using fMRI we first performed independent retinotopic mapping to determine the location of the first three visual areas (V1, V2, and V3). During active visual search we recorded fMRI and behavioural responses to control for differences in visual search performance. Additionally we determined whether the stability of eccentric fixation at the PRL was associated with higher performance and with higher brain activation. Patients with an established PRL should show relatively higher activation in early visual cortex, especially on trials when the target stimuli fell in the vicinity of the PRL.

MATERIALS AND METHODS

Subjects

Twenty-two patients with central scotomata due to hereditary retinal dystrophies (Stargardt's disease, other forms of hereditary macular dystrophies and cone-rod dystrophy, see Table I for details) participated in this study (8 female, 14 male; mean age 41.5 years; range 12–65 years), as well as an age-matched control group of 22 subjects with normal or corrected to normal vision (11 female, 11 male; mean age 42.4 years; range 13–70 years, see Table I for details). Most participants took part in a recent study on structural MRI differences by Plank et al. [2011]. All participants signed an informed consent form prior to the study and received monetary compensation for their participation. The study was approved by the Ethical Committee of the University of Regensburg and conducted in accordance to the ethical guidelines of the Declaration of Helsinki.

Clinical Characteristics and Visual Field Measurements

Table I presents a detailed description of patients and controls, including the diagnosis, duration of disease, visual acuity, scotoma size, fixation stability, and position of PRL in the visual field. All characteristics were measured as described previously [Plank et al., 2011]. All patients had absolute binocular central scotomata with a diameter of at least 10° visual angle or larger and decimal visual acuities of 0.2 or less in both eyes. All controls had a best-corrected decimal visual acuity of 1.0. Best-corrected visual acuity was determined by using a Vision Screener (Rodenstock Rodavist 524/S1) and Eye Charts for distant visual acuity (Oculus Nr. 4616) and near visual acuity (Zeiss/Frohnhäuser). One eye was chosen for stimulation during fMRI measurements and all results are shown for monocular measurements. Those characteristics are given in Table I, the data for the study eye depicted in bold font. Usually the dominant eye was chosen, whereas for five patients (P3, P8, P10, P12, P20) the nondominant eye was chosen, because it was the better eye and/or the one with higher fixation stability. The study eye of the controls was always the eye corresponding to the study eye of their age-matched patient.

Scotoma size was measured using kinetic Goldmann perimetry with the isopters III/4e, I/4e, I/3e, I/2e, and I/1e. Defined as edges of the scotomata, those points were marked, where isopter III/4e were no longer detected. Scotoma size is reported in Table I as scotoma diameter in degrees of visual angle as an average of vertical and horizontal dimensions. Controls did not undergo Goldmann perimetry.

To measure fixation stability of the patients and controls, we used a Nidek MP-1 microperimeter (Nidek Co, Japan). Patients were requested to fixate a red cross of 4 degrees visual angle in diameter with their preferred eccentric location on the retina (PRL) for on average 30 s. Controls fixated the target with their fovea. The technique measures 25 samples per second, so that 750 samples of fixation points result over a time period of 30 s. During the measurement the camera sometimes lost track of the subject's eye. This can be due to eye blinks or fixation instability in the form of large saccades. The Nidek software records the time period that was measured and the

TABLE 1. Characteristics of patients (P1-P22) and controls (C1-C22) according to gender, age, duration of disease in years, diagnosis, decimal visual acuity, scotoma size (diameter in degrees visual angle), fixation stability (percentage of fixation in 2° and 4° visual angle around fixation target; patients fixated with their PRL) and location of PRL in the visual field

					Decimal visual acuity		Scotoma size (diameter in degrees visual angle)		Fixation stability				
									OD		OS		Location of PRL in visual field
Subject #	Gender	Age	Duration of disease in years	Diagnosis	OD	OS	OD	OS	2°	4°	2°	4°	
P1	M	29	5	Stargardt	**0.1**	0.1	**10**	10	**95**	**100**	69	99	Lower
P2	F	25	8	Stargardt	**0.08**	0.05	**20**	25	**20**	**57**	47	64	Lower
P3	M	25	8	Stargardt	**0.1**	0.05	**10**	25	**100**	**100**	20	23	Right
P4	F	35	6	Stargardt	**0.1**	0.1	**10**	10	**98**	**100**	55	97	Left
P5	F	43	9	Stargardt	**0.1**	0.08	**15**	15	**80**	**95**	83	99	Lower
P6	F	43	28	Stargardt	**0.1**	0.1	**10**	10	**26**	**28**	70	93	Lower
P7	M	55	16	Stargardt	**0.1**	0.1	**15**	15	**32**	**59**	52	95	Lower
P8	M	66	13	Stargardt	**0.05**	0.02	**30**	20	**44**	**72**	2	5	Right
P9	M	12	2	Stargardt	0.08	**0.08**	25	**10**	10	46	**62**	**97**	Lower
P10	F	19	9	Stargardt	0.05	**0.05**	n.a.	**15**	7	14	**0**	**2**	Left
P11	F	24	11	Stargardt	0.08	**0.05**	20	**20**	83	100	**86**	**100**	Left
P12	M	39	14	Stargardt	0.05	**0.067**	30	**30**	18	67	**68**	**93**	Left
P13	M	43	24	Stargardt	0.1	**0.1**	20	**20**	58	74	**69**	**77**	Lower
P14	M	45	23	Stargardt	0.1	**0.2**	10	**10**	99	100	**96**	**100**	Lower/left
P15	M	59	16	Cone-rod D	**0.1**	0.1	**10**	10	**20**	**21**	10	18	Lower
P16	M	33	8	Cone-rod D	0.08	**0.08**	25	**25**	47	48	**100**	**100**	Lower
P17	F	41	28	Cone-rod D	0.08	**0.1**	30	**25**	75	96	**83**	**100**	Left
P18	M	65	6	Cone-rod D	0.03	**0.05**	35	**30**	4	9	**78**	**97**	Left
P19	M	65	17	Cone-rod D	0.05	**0.1**	30	**30**	33	81	**43**	**48**	Left
P20	M	50	18	Cone D	**0.1**	0.2	**10**	10	**41**	**69**	42	73	Lower
P21	M	53	23	MD	**0.08**	0.05	**10**	15	**46**	**59**	59	60	Left
P22	F	44	29	CACD	**0.05**	0.067	**10**	25	**15**	**37**	14	50	Lower
C1	M	26	–	–	**1.0**	1.0	–	–	**100**	**100**	n.a.	n.a.	
C2	M	28	–	–	**1.0**	1.0	–	–	**100**	**100**	100	100	
C3	M	23	–	–	**1.0**	1.0	–	–	**100**	**100**	n.a.	n.a.	
C4	F	34	–	–	**1.0**	1.0	–	–	**100**	**100**	99	100	
C5	F	44	–	–	**1.0**	1.0	–	–	**100**	**100**	61	61	
C6	M	45	–	–	**1.0**	1.0	–	–	**96**	**96**	77	77	
C7	F	61	–	–	**1.0**	1.0	–	–	**100**	**100**	100	100	
C8	F	68	–	–	**1.0**	1.0	–	–	**98**	**99**	95	100	
C9	M	13	–	–	1.0	**1.0**	–	–	81	86	**99**	**100**	
C10	F	23	–	–	1.0	**1.0**	–	–	97	100	**98**	**100**	
C11	F	23	–	–	1.0	**1.0**	–	–	n.a.	n.a.	**100**	**100**	
C12	M	43	–	–	1.0	**1.0**	–	–	100	100	**100**	**100**	
C13	M	34	–	–	1.0	**1.0**	–	–	n.a.	n.a.	**100**	**100**	
C14	F	54	–	–	1.0	**1.0**	–	–	89	89	**100**	**100**	
C15	M	60	–	–	**1.0**	1.0	–	–	**100**	**100**	100	100	
C16	M	37	–	–	1.0	**1.0**	–	–	89	89	**100**	**100**	
C17	F	34	–	–	1.0	**1.0**	–	–	n.a.	n.a.	**100**	**100**	
C18	F	62	–	–	1.0	**1.0**	–	–	n.a.	n.a.	**70**	**72**	
C19	M	70	–	–	1.0	**1.0**	–	–	76	77	**97**	**100**	
C20	M	59	–	–	**1.0**	1.0	–	–	**100**	**100**	100	100	
C21	F	55	–	–	**1.0**	1.0	–	–	**100**	**100**	100	100	
C22	F	37	–	–	1.0	**1.0**	–	–	100	100	**96**	**96**	

Bold values indicate values for the study eye that was chosen during the fMRI measurements.
m, male; f, female; Stargardt, Stargardt's disease; CACD, central areolar choroidal dystrophy; MD, unclassified hereditary macular dystrophy; Cone D, cone dystrophy; Cone-rod D = cone-rod dystrophy; OS, oculus sinister; OD, oculus dexter; characteristics of the better eye of each patient are reported in bold, that are correlated with MRI data. For the controls the respective eye was chosen.

proportion of the time span that was effectively tracked, as well as the percentages of fixation points that fell in a range of 2° or 4° diameter visual angle around the center of the target, based on the time spans effectively tracked. Thus fixation stability can be overestimated by long or frequent time spans where the camera lost track of eye position due to large saccades. To compensate for this we corrected the given fixation stability as described in Plank et al. [2011]. These corrected values are given in Table I. Figure 1 (upper panel) presents examples from a patient with stable fixation (A) and one with less stable fixation (B), respectively.

The Nidek MP-1 was also used to measure a microperimetry of 30 degrees diameter around the patients' PRL. Patients fixated a central cross with their PRL on intact retina and were instructed to press a button as soon as they perceived a target. Controls also underwent microperimetry and fixated the central cross with their fovea. We used "strategy-fast" with static light points of intensity 16 and 8 dB, maximal brightness of 127 cd/m^2, that were presented for 200 ms each on a grid comprising the central 30° of the visual field.

We determined the position of PRLs according to the resultant Nidek images. This was later verified using a video eyetracker (High Speed Video Eyetracker Toolbox, Cambridge Research Systems, UK), while the participants fixated a central target on a computer monitor. Eight participants had a PRL located in the left visual field, 11 participants used a PRL in the lower visual field, two participants a PRL in the right visual field. One participant (P 14) used two different PRLs deliberately for certain tasks, one in the lower visual field for reading and one in the left visual field for looking at objects. For the analysis here we only considered the PRL in the lower visual field of patient 14 that seemed more appropriate for our visual search task. Figure 1 (lower panel) presents an overview of the location of the PRLs of Patients 1–22, who participated in the current experiment.

Stimuli and Procedure

The results reported here are part of a larger follow-up study, in which participants underwent structural and functional MRI measurements and every subject completed three sessions over an interval of 6 months. The functional MRI measurements consisted of retinotopic mapping paradigms, a direct stimulation of patients' PRL and two visual search tasks completed in each session. Here we primarily report the results of the visual search task obtained in one of the three sessions. Usually the data of the first session are reported. For four patients the visual search results of the second or third session are reported (P5: session 2; P9: session 3, P10: session 2; P19: session 2) due to a still developing PRL in the time course of the study or lack of clarity about the exact location of the PRL in former sessions. Additionally meridian mapping was employed to functionally determine the locations of visual areas V1, V2 and V3 for each participant. All other results will be reported elsewhere. Visual stimuli were projected onto a circular screen (31° visual angle in diameter at a distance of 60 cm) placed behind the head of the participant at the end of the scanner bore and visible via a mirror placed within the MRI head coil. All visual sequences were presented with the software Presentation (Neurobehavioral Systems Inc.) and triggered by the scanner signal. The participants conducted all paradigms with their study eye, the other eye was patched during the measurement. All participants had to fixate with their fovea at the center of the screen during all tasks. Controls simply did that by fixating foveally a central fixation target (the letter "X"). For patients with central visual field scotomata we presented auxiliary stimuli to ensure fixation. Depending on how well they could consciously perceive their scotoma and/or how well they were accustomed to fixate with their PRL, these auxiliary stimuli were adapted to the individual needs of the patients. The auxiliary stimuli consisted of four red dots (each about .7° visual angle in diameter) positioned at the edges of the respective scotoma and/or the fixation target (letter "X") at the position of the PRL (Fig. 2). The fixation target was located at a position in the visual field that corresponded to the PRL and was adapted in size to the needs of the patients (between .95° and 2.1° visual angle). The correct adaptation of the position of the auxiliary stimuli on the screen and the direction of gaze was controlled prior to scanning by using a video eyetracker (High Speed Video Eyetracker Toolbox, Cambridge Research Systems, UK) under comparable viewing conditions as during fMRI. Fixation inside the scanner was monitored in most patients using an MR-Eyetracker [Kimmig et al., 1999]. Although some of the patients were not able to fixate with their PRL as well as controls fixated with their fovea, we employed the MR-Eyetracker to monitor systematic meanderings of gaze during task conditions. Behavioral data analyses included analysis of response speed (reaction times) and performance (sensitivity index d' from signal detection theory). Those seldom d' values which were not determinable due to 100% correct or 0% false alarms were estimated by adding or subtracting 0.5 observations to an otherwise empty cell of the pay-off matrix [Kadlec, 1999; Wickens, 2002].

Visual Search Task

During the search task, participants were presented with white letters (330 cd/m^2) on a dark screen (1 cd/m^2); letters "L" and "T" were arranged in two eccentric circles (see Fig. 2). The inner circle comprised a range of 12–16.2° visual angle in diameter, the outer circle a range of 18.1–24.1° visual angle in diameter. The letters were scaled in size (letters in the inner circle: 2.2° visual angle; letters in the outer circle: 2.9° visual angle) and randomly shifted against each other on each trial. This spatial jitter was

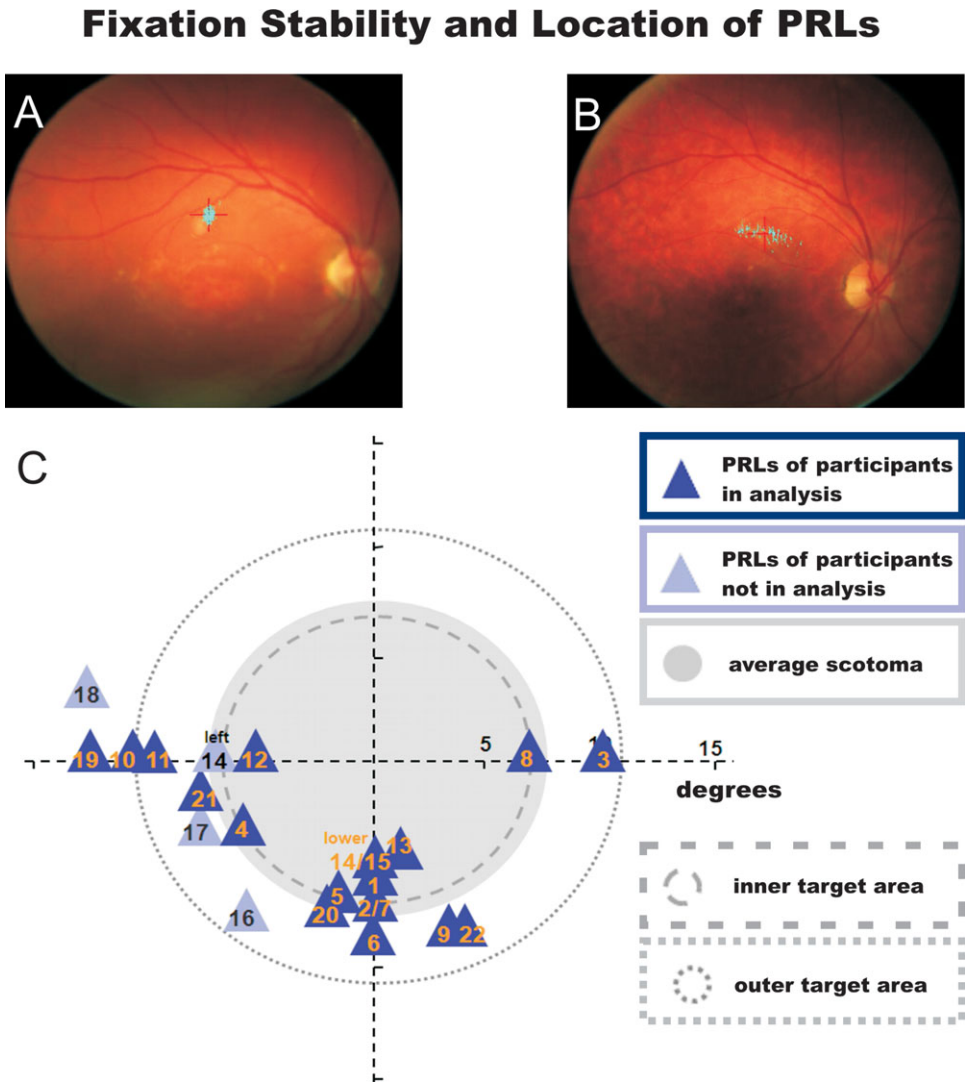

Figure 1.

Upper panel: Examples of fixation stability measurements with the Nidek MP-1 microperimeter: (**A**) for the right eye of a patient exhibiting fairly stable fixation (P1) and (**B**) for the right eye of a patient with less stable fixation (P2, see Table 1). The patients fixated with their PRL eccentrically on a red cross for 30 s. The aquamarine colored dots represent samples of fixation points on the retina during that time period. Lower panel: Schematic depiction of positions of PRLs for all patients (numbered from 1 to 22), who were able to perform the visual search task. The *x*- and *y*-axis of the plot give the eccentricity in degrees of visual angle. The filled gray circle depicts the size of the average scotoma in our patient sample, the dashed and dotted circles give the position of the center of the two rings where target and distractor stimuli were presented. The triangles give the positions of patients' PRLs. The dark blue triangles show all PRLs of patients included in the analysis, the light blue triangles show PRLs of patients excluded from the analysis, because they had large, asymmetrical scotomata leading to large blind areas in the opposite hemifield (see Methods and Results section for a description of exclusion criteria). Patient 14 had developed two PRLs, one in the left visual field and one in the lower visual field. Since he used the PRL in the lower visual field for reading, which comes close to the letter identification task in this study, we included his PRL in the lower visual field in the analysis and excluded the one in the left visual field, which he uses primarily for looking at faces or objects.

used to avoid that the distractor letters ("Ts") along the inner circle and their counterparts on the outer circle formed a collinear pattern which would render the target stimuli ("Ls") more salient (Fig. 2).

On each trial participants were requested to detect the letter "L" whenever it was presented amongst letter-T distractors, and press a button to acknowledge that he/she had seen the letter "L". Responses were recorded with a 5-

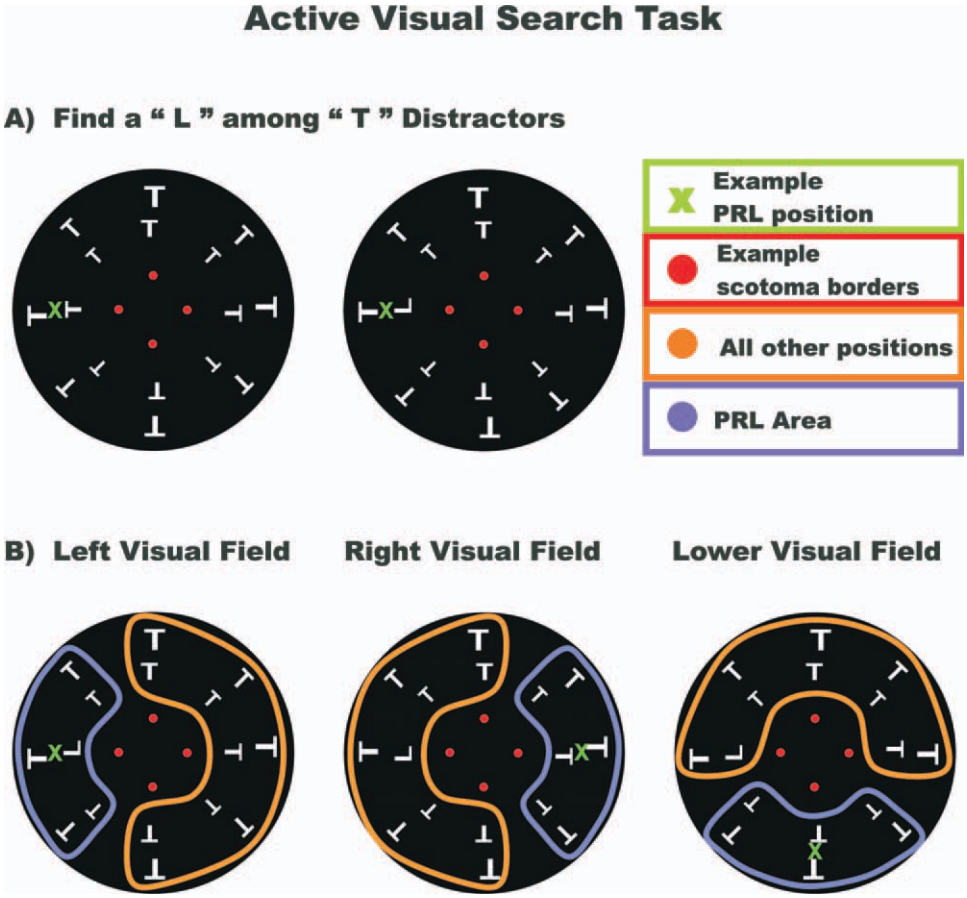

Figure 2.

A: Examples of stimulus arrangements in a "target absent" trial (left) and a "target present" trial (right). Participants were requested to detect if the target letter "L" was present at any position between radially arranged distractor letters "T". Auxiliary stimuli consisting of four red dots at the borders of the scotoma and/or a fixation target in form of a green letter "X" at the location of a patient's PRL helped the JMD patients to maintain fixation during the task. For controls the fixation target "X" was positioned at the center of the screen. **B**: Schematic depiction of how target positions were pooled in the analysis of the results. Differences in hit rates, reaction times, and percent BOLD signal changes were calculated between trials with target stimuli in the vicinity of patients' PRLs (PRL area, six positions, marked by the purple borders, which are shown here for purpose of illustration and were never present in the experiments) and trials with target stimuli at all other positions outside their PRL area (10 positions, marked by orange borders). Thus we defined the PRL areas for our groups of patients with their PRL in the left, right or lower visual field. [Color figure can be viewed in the online issue, which is available at wileyonlinelibrary.com.]

button fiber-optic response box (Lumitouch, Photon Control, Ltd, Burnaby, BC, Canada). The stimuli were presented for 500 ms and there was a blank period of 2 s between each trial. In total 256 trials were performed by each participant. Half of the trials (n = 128) contained a single target (letter "L") amongst 15 distractors (letter "T"), the other trials contained 16 distractors and no target. The position of the target was pseudo-randomized for all 16 positions (eight trials per position). The control subjects were asked to fixate with their fovea at the center of the screen. Similarly, for patients, we asked them to view the display with their PRL in such a manner (for individual cases) that their scotoma is centered in the middle of the screen. As for meridian mapping (see below) this was achieved by placing four red 0.7 deg dots at the borders of each patient's scotoma or by placing an appropriately sized letter X at the position of the patients' PRL in the visual field.

Visual search control task

In a control task, on each trial a single letter "L" or "T" was presented in the absence of distractors at only one of the 16 positions indicated in Figure 2, and additionally at the central position. The control task was also conducted in the MR scanner under the same conditions as the visual

search task. While subjects fixated foveally at the center of the screen, they should indicate by button press, which of the two letters they had seen. If they failed to detect a letter at any of the given positions, they were instructed not to respond, counting the trial as a miss. A trial lasted for 500 ms with an inter-trial interval of 2 s. A total of 146 trials were completed. This paradigm allowed us to test the L/T-discriminability in different parts of the visual field with high contrast stimuli as were used in the main visual search task. These stimuli often were still reported by the patients in parts of the visual field that were otherwise indicated as belonging to the scotoma in the Goldmann perimetry (see Results section).

Meridian mapping

In this paradigm we measured the cortical responses to the presentation of flickering checkerboards covering the horizontal and vertical meridian with the goal to identify the borders of the retinotopic areas V1, V2 and V3 [Beer et al., 2009; DeYoe et al., 1996]. Black (1 cd/m^2) and white (330 cd/m^2) checkerboard stimuli with a flicker rate of 8 Hz were presented sequentially, covering the horizontal and vertical meridian, on a gray background of mean luminance in a block design together with a baseline condition of mean luminance. The blocks were presented in eight cycles. Flickering checkerboards were presented in blocks of 19 s, the baseline condition (i.e., blank screen) in blocks of 18 s. The auxiliary stimuli (red dots) and fixation target (the letter X) were visible throughout the stimulation for all participants. The representations of the horizontal and vertical meridians on the visual cortex were then identified by computing the contrast between the horizontal vs. vertical wedge positions. Vertical meridian representations marked the borders between V1 and V2, and horizontal meridian representations marked the borders between V2 and V3. The borders between dorsal and ventral were set at the midline of the representation of the horizontal meridian coinciding with the calcarine sulcus.

MRI Data Acquisition

Scanning was performed on a research-dedicated Siemens Allegra 3-Tesla head scanner with a single channel headcoil. Functional images were acquired using a T2*-weighted gradient echo-planar imaging (EPI) sequence (TR = 2 s, TE = 30 ms, 34 slices, FoV = 192 × 192 mm^2, flip angle = 90°, 3 × 3 × 3 mm^3 voxel size). The axial slices were oriented parallel to the line connecting the anterior and posterior commissure and covered the whole brain. Two dummy scans at the beginning of each measurement were removed automatically from the data set.

Additionally a high-resolution T1-weighted image (160 sagittal slices covering the whole brain, 1 × 1 × 1 mm^3 voxel size, FOV = 256 × 256 mm^2) was obtained from each subject, using the ADNI sequence (TR = 2250 ms, TE = 2.6 ms, flip angle 9°; Laboratory for Neuro-Imaging, UCLA, Los Angeles, CA).

MRI Data Analysis

Cortical reconstruction

The T1-weighted structural image obtained from each subject was reconstructed by Freesurfer version 4.1 (Martinos Center for Biomedical Imaging, Charlestown, MA) as described in Beer et al. [2009, 2011]. The cortical reconstruction procedure included the removal of nonbrain tissue with a hybrid watershed/surface deformation procedure [Segonne et al., 2004], correction for intensity nonuniformities [Sled et al., 1998], and automatic transformation into Talairach space. After segmentation of the subcortical white matter and deep gray matter volumetric structures [Fischl et al., 2002, 2004b], the gray-white matter boundary was tessellated and topologic inaccuracies automatically corrected [Fischl et al., 2001; Segonne et al., 2007]. The surface was then deformed following intensity gradients to optimally place the gray/white and gray/cerebrospinal fluid borders at the location where the greatest shift in intensity defines the transition to the other tissue class [Dale et al., 1999; Fischl and Dale, 2000]. Once the cortical models were complete, the cortical surface was inflated [Fischl et al., 1999a], registered to a spherical atlas which utilized individual cortical folding patterns to match cortical geometry across subjects [Fischl et al., 1999b], and automatically parcellated into units based on gyral and sulcal structures [Desikan et al., 2006; Fischl et al., 2004b]. Finally we created an occipital flat patch of the inflated surface posterior to the sylvian fissure (cut along the calcarine sulcus).

Preprocessing of functional data

Data analysis was performed with the FS-Fast tools of Freesurfer. Preprocessing steps included motion correction [Cox and Jesmanowicz, 1999], coregistration to the anatomical image acquired in the same session, smoothing with a Gaussian kernel of 5 mm FWHM and correction for intensity nonuniformities [Sled et al., 1998]. Additionally, the first volume of each session was automatically coregistered to the structural volume and manually verified (and corrected) using visual ("blink") comparison.

Statistical Data Analysis and ROI Labeling

Meridian mapping

To obtain functional estimates of the anatomical borders between visual areas V1 and V2 as well as between V2 and V3 we contrasted conditions of horizontal meridian representations with vertical meridian stimulations [see also Beer et al., 2009]. Statistical parametric maps were calculated based on the general linear model using the

stimulation blocks convoluted with a cumulative gamma function (with parameters: delta = 2.25; tau = 1.25; alpha = 2) as predictors. Additionally, linear and cubic predictors (modeling slow signal drifts) and motion correction parameters were added to the design matrix. Significance maps for each contrast were then overlaid on the flattened cortical surface of each individual hemisphere. On these flat maps, the borders between dorsal and ventral were set at the midline of the representation of the horizontal meridian coinciding with the calcarine sulcus, the borders between V1/V2 and V2/V3 were set at the midline of the representations of the vertical and horizontal meridian, respectively. The obtained ROIs V1d/v, V2d/v, and V3d/v of each hemisphere were used for the subsequent ROI analysis (see Fig. 5, upper panel).

Visual Search Task

The visual search task was analyzed by the general linear model adopting an event-related design. Stimulus events were convolved with a gamma function (with parameters: delta = 2.25; tau = 1.25; alpha = 2). Additionally, a linear and cubic predictor and motion correction parameters were added to the design matrix. The stimulus sequence contained 17 conditions. Conditions 1-16 consisted of trials, where the target letter "L" appeared in one of the 16 positions respectively (eight trials per position). Condition 17 contained all 128 nontarget trials. Statistical analysis was restricted to the ROIs V1d/v, V2d/v, and V3d/v of each hemisphere (see above). Of all functional voxels falling within each ROI the mean BOLD signal change (in percent) was calculated for each condition. Subsequently, at each of the 16 target positions, we determined the difference of percent signal change in trials where the target letter "L" was present in comparison to percent-signal change in "target-absent" trials. We then calculated mean BOLD signal changes of these differences in the respective retinotopic representation areas in visual cortex for the PRL area (comprised of six possible target positions as depicted in the purple framed area in Fig. 2) and in the same way for "all other positions" (comprised of the remaining ten positions within the orange framed area in Fig. 2). The differential mean BOLD signal changes were pooled across the left and right hemispheres or across dorsal and ventral areas of V1, V2, and V3, when appropriate for the analyzed target positions.

RESULTS

Behavioural Results

Single letter presentation: control task

To measure the distribution of sensitivity in the visual field for our patients for the high contrast letters we employed in our visual search task, we measured hits and misses in the single-letter control task. Here we were only interested in the patients' ability to discriminate between the presence of the letter L or T alone. For all patients, especially those with large scotoma (20° visual angle in diameter or larger; P2, P8, P11, P12, P13, P16, P17, P18, P19), we determined the percentage of misses in all 16 positions along the two rings. We recorded the miss rate for the 10 positions that covered the Non-PRL-area to avoid a bias in our results in favor of principal sensitivity in the PRL area. Subsequently we excluded any patients from further analysis, for whom the miss rate in all 16 outer positions and/or in the Non-PRL-area exceeded 60%. According to this analysis, three of our patients with large scotomata (P16, P17, P18) had to be excluded from further analysis. Their collected behavioural and fMRI data were retroactively discarded. The remaining patients showed a mean hit rate in the PRL area of 78.3% correct (SE = 4.8) and in all other positions of 70.7% correct (SE = 5.6). These two hit rates differed significantly from each other ($P = .034$). The mean hit rate of the central position was 24.8% correct (SE = 7.1). Controls had a mean hit rate of 96.1% correct (SE = 0.89), false alarms of 3.3% (SE = 0.89) and mean misses of 0.6% (SE = 0.19) over all positions and no single positions differed significantly from the others.

Visual Search Task

As described in the methods section, we assigned six positions in or near the "PRL area" (Fig. 2), and an area comprising "all other positions" (10 positions), and calculated hit rates and reaction times accordingly for these two areas for each participant. After excluding patients P16, P17, and P18 (due to the exclusion criteria noted above), six patients made up the left visual field PRL group, 11 patients formed the lower visual field group and two patients defined the right visual field PRL-group. We calculated global hit rates (percentages of correct responses) for the "PRL area" and "all other positions" (see Fig. 2) and transformed those to sensitivity measures of d'. Patients exhibited significantly higher mean hit rates (measured in d') [mean $d' = 1.42$; SE = 0.18] in their PRL area than on average at all other positions [mean $d' = 0.91$; SE = 0.18] outside the PRL area [$t(18) = 3.74$; $P = 0.001$]. For the controls we also defined a "PRL area" arbitrarily in accordance to the PRL area of their corresponding age-matched patient and calculated the hit rates respectively. As expected, performance measures for the controls did not differ significantly between the arbitrarily assigned "PRL area" [mean $d' = 2.22$; SE = 0.2] and "all other positions" [mean $d' = 2.18$; SE = 0.18] [$t(21) = 0.48$; $P = 0.64$]. A repeated-measures ANOVA on the within-subject-factor "position" (PRL area vs. all other positions) and the between-subject-factor "group" (patients vs. controls), revealed a significant main effect of "position" [$F(1,39) = 12.4$; $P = 0.001$], a significant main effect of "group" [$F(1,39) = 16.3$; $P < 0.001$], as well as a significant interaction between the factors "position" and "group" [$F(1,39) =$

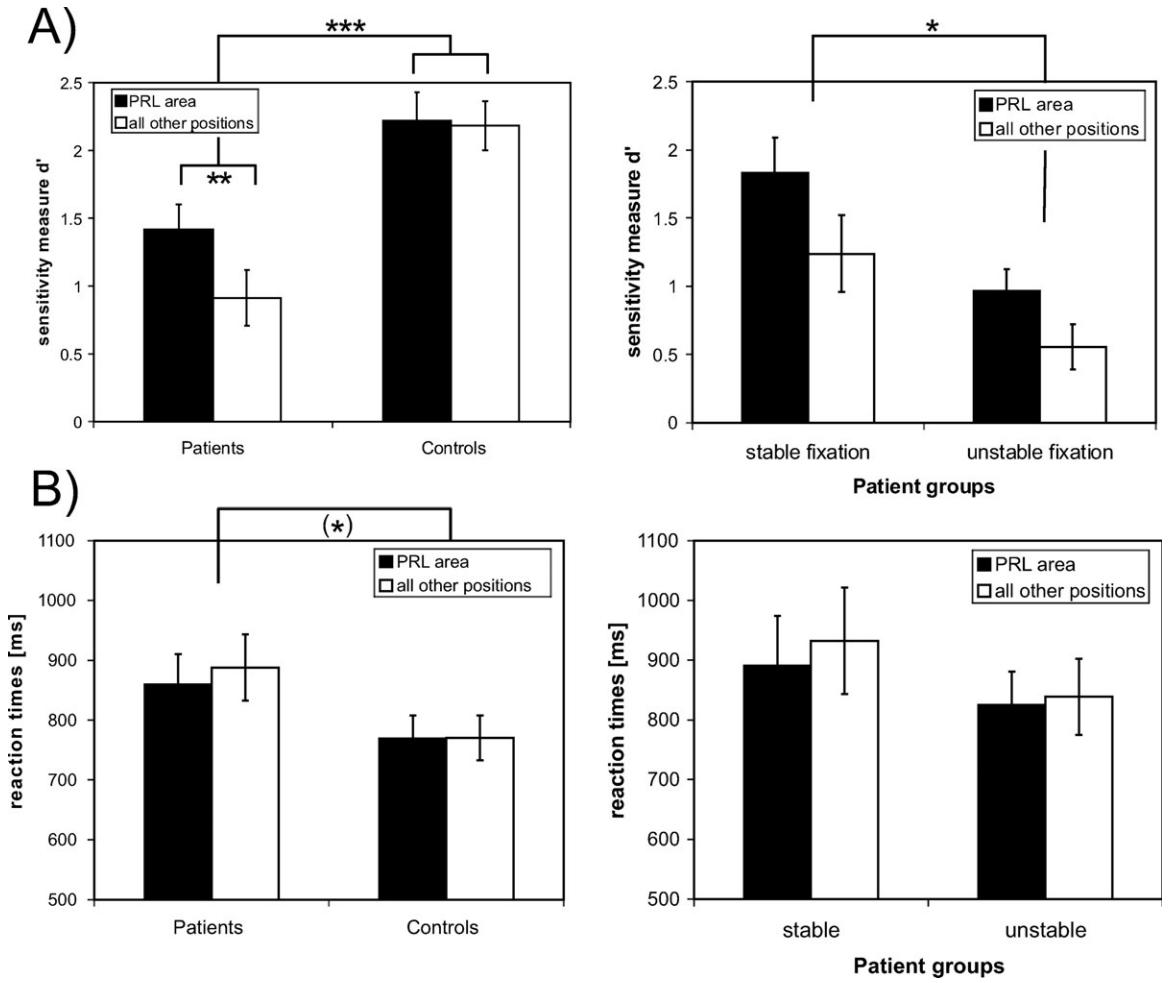

Figure 3.

Behavioural group results in the visual search paradigm. **A**: Performance, measured with *d'*, together with the respective standard errors for the patient and control group (left) and within the patient sample plotted separately for the group with stable fixation and with unstable fixation (right). **B**: Mean reaction times (in ms) together with the respective standard errors for the patient and control group (left) and within the patient sample for the group with stable fixation and with unstable fixation (right). Dark columns represent *d'* for trials where the target appeared at one of six positions in the PRL area, white columns represent *d'* for trials where the target appeared at any other of ten positions outside the PRL area. Marked with stars (*) are those columns, which differed significantly from each other [significance levels: ***$P < 0.001$; **$P < 0.01$; *$P < 0.05$; (*) $P < 0.1$].

8.9; $P = 0.005$]. Figure 3, Panel A illustrates these results. Patients showed significantly lower hit rates than controls, and only in the patients group a difference in hit rates between PRL area and other positions could be found. The false alarm rate (i.e., where participants responded that a target was present on a nontarget trial) was 13.65% for the patients and 8.95% for the controls.

The data for the factor level "all other positions" were pooled over a larger number of positions than for the factor level "PRL area", which could have biased the results. To account for this we conducted an additional analysis, where we compared the "PRL area" to an equal number of six positions in the opposite hemifield of each PRL group. For this we excluded the two positions on the vertical meridian for the groups with their PRL in the left or right visual field, and the two positions on the horizontal meridian for the group with the PRL in the lower visual field. A repeated-measures ANOVA on the within-subject-factor "position" (PRL area (six positions) vs. opposite hemifield (six positions)) and the between-subject-factor "group" (patients vs. controls), revealed almost identical results to the former analysis: a significant main effect of "position" [$F(1,39) = 8.47$; $P = 0.006$], a significant main effect of "group" [$F(1,39) = 16.35$; $P < 0.001$], as well as a significant interaction between the factors "position" and "group" [$F(1,39) = 8.98$; $P = 0.005$].

Role of fixation stability in the visual search task

To examine the role of fixation stability we split our patient sample at the median value (45.78%) of the fixation stability measured in an area around 2° visual angle (see Table I), that gives a narrower range for fixation stability than the measures in an area around 4° visual angle. All patients with a fixation stability ≥ the median value were assigned to the group with stable fixation ($n = 10$), all other patients with a fixation stability < the median value were assigned to the group with unstable fixation ($n = 9$). We calculated the hit rate and the corresponding d' value at the PRL area and at all other positions separately for these two fixation groups. A repeated-measures ANOVA with the within-subject factor position (PRL vs. all other positions) and the between-subject factor fixation stability (stable vs. unstable) revealed a main effect of position [$F(1,17) = 13.2$; $P = 0.002$] and of fixation stability [$F(1,17) = 6.9$; $P = 0.018$]. The interaction was not significant [$F(1,17) = 0.4$; $P = 0.54$] (see Fig. 3, Panel A). These differences in performance appear to be unrelated to scotoma size, since the two fixation groups did not differ significantly in scotoma size: the group with stable fixation had a mean scotoma size of 14.5° visual angle (SE = 2.2), the group with unstable fixation had a mean scotoma size of 16.7° visual angle (SE = 2.8) [$t(17) = -0.62$; $P = 0.54$].

Additionally we performed post-hoc pairwise comparisons to address performance differences between controls and the two patient groups with stable and unstable fixation separately. Those tests revealed that performance of the patient group with stable fixation did not differ significantly from the controls' performance, when the target appeared around their PRL [$P = 0.54$; Bonferroni corrected for multiple comparisons]. For targets appearing at any other position in the visual field, patients with stable fixation performed significantly worse than controls [$P = 0.014$; Bonferroni corrected for multiple comparisons]. Patients with unstable fixation performed significantly worse than controls in both cases, for trials with the target around their PRL [$P = 0.002$; Bonferroni corrected for multiple comparisons] as well as for trials with the target at any other position [$P < 0.001$; Bonferroni corrected for multiple comparisons]. It is noteworthy though to add that, despite the differences in performance, the d'-values in all groups and all conditions differed significantly from zero ($P < 0.05$), indicating that on average participants of all groups were capable of doing the task, with performances clearly above chance level.

Also in this analysis we conducted an additional repeated-measures ANOVA with the within-subject factor position [PRL area (six positions) vs. opposite hemifield (six positions)], to account for equal number of positions pooled, and the between-subject factor fixation stability (stable vs. unstable). It revealed a main effect of position [$F(1,17) = 11.01$; $P = 0.004$] and of fixation stability [$F(1,17) = 7.4$; $P = 0.015$]. The interaction was again not significant [$F(1,17) = 0.4$; $P = 0.54$].

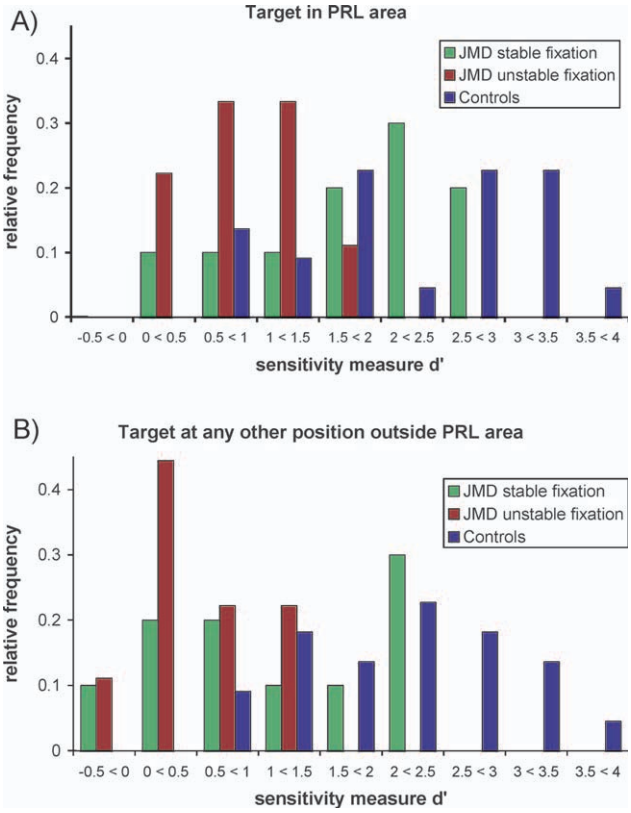

Figure 4.

Relative frequency of observations as a function of the performance level (d') for the patients with unstable fixation (red columns), for the patients with stable fixation (green columns) and for the controls (blue columns). [Color figure can be viewed in the online issue, which is available at wileyonlinelibrary.com.]

To emphasize the group differences in performance we plotted the distribution of relative frequencies for the two patient groups with stable and unstable fixation and the control group. Figure 4, Panel A shows that in trials with target stimuli appearing in the PRL area, patients with unstable fixation mostly showed d' values between 0.5 and 1.5, while patients with stable fixation mostly showed d' values between 1.5 and 3. In trials with the target stimuli appearing at any position outside the PRL area (Fig. 4, Panel B), patients with unstable fixation mostly showed d' values between 0 and 1.5, while the performance of patients with stable fixation were equally distributed between 0 and 2.5. In comparison, performance levels for the controls lie between d' values of 0.5 and 4, with a peak around d' values between 2 and 3.

Reaction times

Figure 3 Panel B presents the results from the reaction time analysis for the patient and control group. We considered again mean reaction times for targets presented in

the PRL area in contrast to targets presented at all other positions. A repeated-measures ANOVA on the within-subject factor "position" (PRL area vs. all other positions) and the between-subject factor "group" (patients vs. controls) revealed a significant main effect of "position" [$F(1,39) = 4.54$; $P = 0.039$]. The main effect "group" was marginally significant [$F(1,39) = 3.4$; $P = 0.073$]. The interaction between the two factors was not significant [$F(1,39) = 1.9$; $P = 0.175$]. Additionally we examined the effects of fixation stability on reaction times. A repeated-measures ANOVA was performed on the same groups with stable and unstable fixation as described above, and with the within-subjects factor "position" (PRL area vs. all other positions), see Figure 3, Panel B. The analysis revealed a significant main effect of "position" [$F(1,17) = 8.9$; $P = 0.008$]. The main effect "fixation stability" was not significant [$F(1,17) = 0.552$; $P = 0.47$], as well as the interaction between the two factors [$F(1,17) = 2.43$; $P = 0.137$].

fMRI Data

Meridian mapping

Figure 5 (upper panel) presents the results of the meridian mapping in a representative patient and control. Statistical parametric maps of the BOLD response were overlaid on the respective individual occipital cortices of the right hemisphere in the form of an inflated gray matter surface and a flat map.

Horizontal and vertical meridian stimulation yielded stripes of activation parallel to the calcarine sulcus that allowed us to draw the borders between V1 and V2 (vertical meridian) as well as between V2 and V3 (horizontal meridian). Dorsal and ventral parts of the visual areas were separated anatomically by placing a line through the calcarine sulcus corresponding to the midline of the activation elicited by the horizontal meridian stimulation in this area. Although activation in the foveal representation area was usually missing in the patient group due to their central scotomata the remaining information was sufficient to determine the borders between visual areas in all but two (P8 and P14) participants. Table II shows the mean sizes of the ROIs for both hemispheres for the patient and control group determined in this fashion. There were no statistically significant differences in the sizes of the ROIs between the patient and control groups, with the exception of V1v of the right hemisphere ($P = 0.04$), where the patients showed a slightly larger cluster of activation.

Visual search paradigm

ROI Analysis for V1, V2, and V3—comparison between patients and controls. We were interested in differences in brain activation in retinotopic areas V1, V2, and V3 between the patient and control group while they performed the visual search task. Here we examined especially the PRL projection zone in comparison to

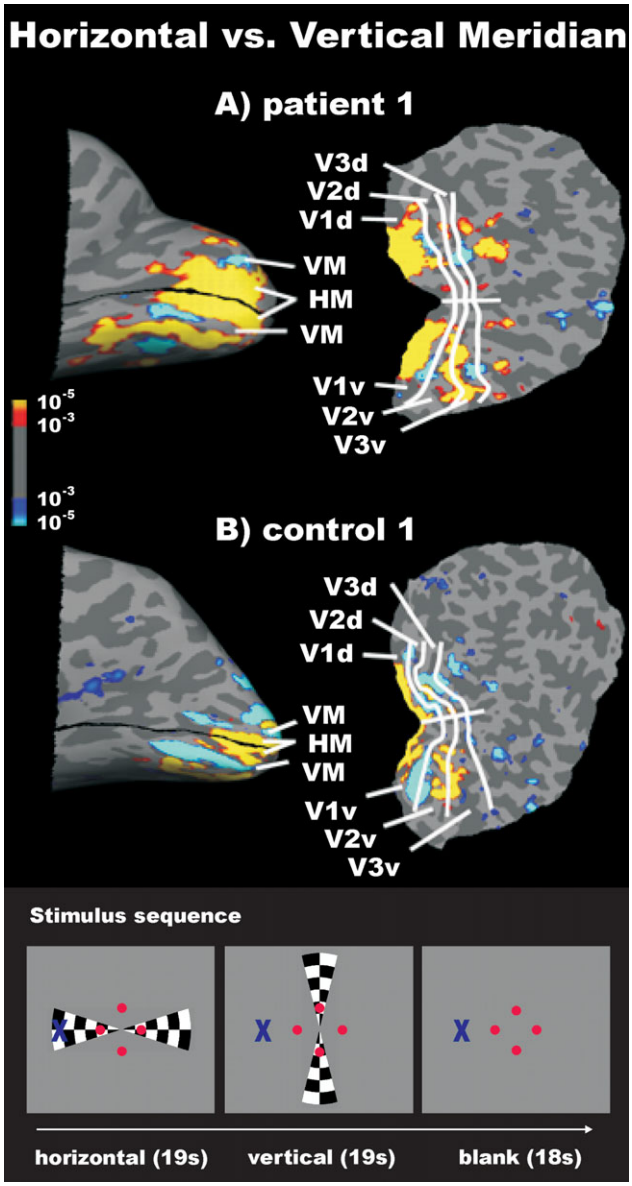

Figure 5.

Upper Panel: Results of meridian mapping and definition of ROIs in a sample patient (P1) and corresponding sample control (C 1). Horizontal (HM, yellow) and vertical (VM, blue) meridian representations are shown on an inflated gray matter surface (left) and a flat patch (right) of the occipital cortex, cut through the calcarine sulcus, of the right hemisphere. Color bars represent *P*-values. On the basis of the meridian representations visual areas V1d, V1v, V2d, V2v, V3d, and V3v could be separated. Lower panel: Stimulus arrangement in the meridian-mapping paradigm. Blocks with flickering checkerboards stimulating the horizontal and vertical meridian alternated with blank baseline blocks of mean luminance. Auxiliary stimuli (red dots at scotoma borders and/or fixation target "X" at the position of patients' PRLs) helped the patients to maintain central fixation. For controls the fixation target was set at the center of the screen. For comparability, red dots were also present for controls.

TABLE II. Sizes of ROIs, given in number of significantly active functional voxels (3 × 3 × 3 mm^3), determined in the patient group as a mean of 20 participants, and from the control group as a mean of 22 participants, together with their respective standard errors (SE) for the left and right hemisphere

		Left hemisphere		Right hemisphere	
ROI	*n*	Size	SE	Size	SE
Patients					
V1d	20	235.4	21.48	230.8	15.19
V1v	20	195.2	17.63	218.7	16.03
V2d	20	260.8	17.05	260.0	18.02
V2v	20	194.5	13.01	220.3	16.22
V3d	20	301.1	24.42	290.4	20.82
V3v	20	206.8	12.39	238.3	15.75
Controls					
V1d	22	214.3	13.10	200.7	8.64
V1v	22	165.6	9.85	178.9	9.47
V2d	22	289.0	18.90	231.9	13.27
V2v	22	204.9	12.29	232.1	14.30
V3d	22	297.9	20.26	266.1	14.57
V3v	22	200.7	12.50	243.4	15.85

In the patient group, visual areas V1, V2, and V3 could not be determined in two patients (P8 and P14) due to low levels of BOLD response.

representation areas of "all other positions" in target present vs. target absent trials. Thus, for the group of patients with the PRL in the lower visual field and their respective controls, we considered BOLD activation in the dorsal portions only, pooled over both hemispheres, as the PRL projection zone, and ventral portions only as representation area of "all other positions," also pooled over hemispheres. For the patients with the PRL in the left visual field and their respective controls, we considered BOLD activation in the right hemisphere only as the PRL projection zone and BOLD activation in the left hemisphere only for "all other positions," pooled over dorsal and ventral portions. For the two patients with their PRL in the right visual field and their controls, we considered BOLD activation in the left hemisphere only for the PRL projection zone and in the right hemisphere only for "all other positions," again pooled over dorsal and ventral portions. As described above, patients P16, P17, P18 were also excluded from this analysis, as well as patients P8 and P14, for whom the borders between visual areas could not be determined. To calculate the mean values for the condition "target in PRL zone" and for the condition "target in all other positions," percent signal change values were always pooled over the respective target positions as depicted in Figure 2B. A repeated-measures ANOVA with the three within-subject factors "target present vs. target absent," "target position" (PRL zone vs. all other positions) and "visual area" (V1, V2, V3) and the between subject factor "group" (patient vs. control) was computed with respect to the dependent variable "percent signal change". This analysis yielded no significant main effects (all $P > 0.05$), but a significant interaction between the factors "target present vs. target absent" and "group" [$F(1,37) = 5.12$; $P = 0.03$]. All other interactions were not significant ($P > 0.05$). Therefore we tested the patient and control groups separately. The repeated-measures ANOVA with the same within-subject factors as above within the control group revealed no significant main effects or interactions (all $P > 0.05$). The ANOVA within the patient group revealed a significant main effect of "target present vs. target absent" [$F(1,16) = 6.85$; $P = 0.019$] with significantly higher BOLD responses in the "target present trials". The main effects "target position" [$F(1,16) = .29$; $P = 0.6$] and "visual area" [$F(2,32) = 1.95$; $P = 0.16$] were not statistically significant, nor were any interactions statistically significant ($P > 0.05$). A similar result was obtained when we conducted the same ANOVA under consideration of an equal number of positions pooled for the "PRL area" (six positions) and the "opposite hemifield" (six positions). It also revealed a significant main effect of "target present vs. target absent" [$F(1,16) = 6.01$; $P = 0.026$]. The main effects "target position" [$F(1,16) = 0.34$; $P = 0.57$] and "visual area" [$F(2,32) = 1.83$; $P = 0.18$] were again not statistically significant, nor were any interactions statistically significant ($P > 0.05$).

Additionally we tested the mean differences in percent signal change between "target present" and "target absent" trials with respect to their difference from zero. This analysis indicated that patients only exhibited significant BOLD response differences differences on trials with targets in the PRL zone, for all three visual areas V1, V2, and V3 (see Fig. 6A, indicated by stars; $P \leq 0.05$). The same result holds when we consider % signal change values pooled over six positions in the opposite hemifield only instead of pooled over "all other positions".

ROI analysis for V1, V2, and V3—role of fixation stability in the patient group. To explore the role of fixation stability further, we computed the same ANOVA separately for the patient groups with stable fixation and with unstable fixation. In the group with stable fixation this analysis revealed a significant effect of "target present vs. target absent" trials [$F(1,8) = 9.7$; $P = 0.014$] and additionally a significant main effect of "target position" [$F(1,8) = 5.8$; $P = 0.042$], with higher percent signal change values in trials where the target fell in the PRL zone. Thus the BOLD response appears to be significantly up-regulated when a target appeared in the PRL projection zone in comparison to nontarget trials, an effect completely absent in controls (Fig. 6). The main effect "visual area" as well as all interactions were not statistically significant (all $P > 0.05$). In the group with unstable fixation on the other hand all main effects and interactions yielded no significant results. Figure 6B illustrates these results as mean percent signal change values for patient groups with stable and unstable fixation. For viewing convenience we plotted the difference between "target present" and "target absent" trials.

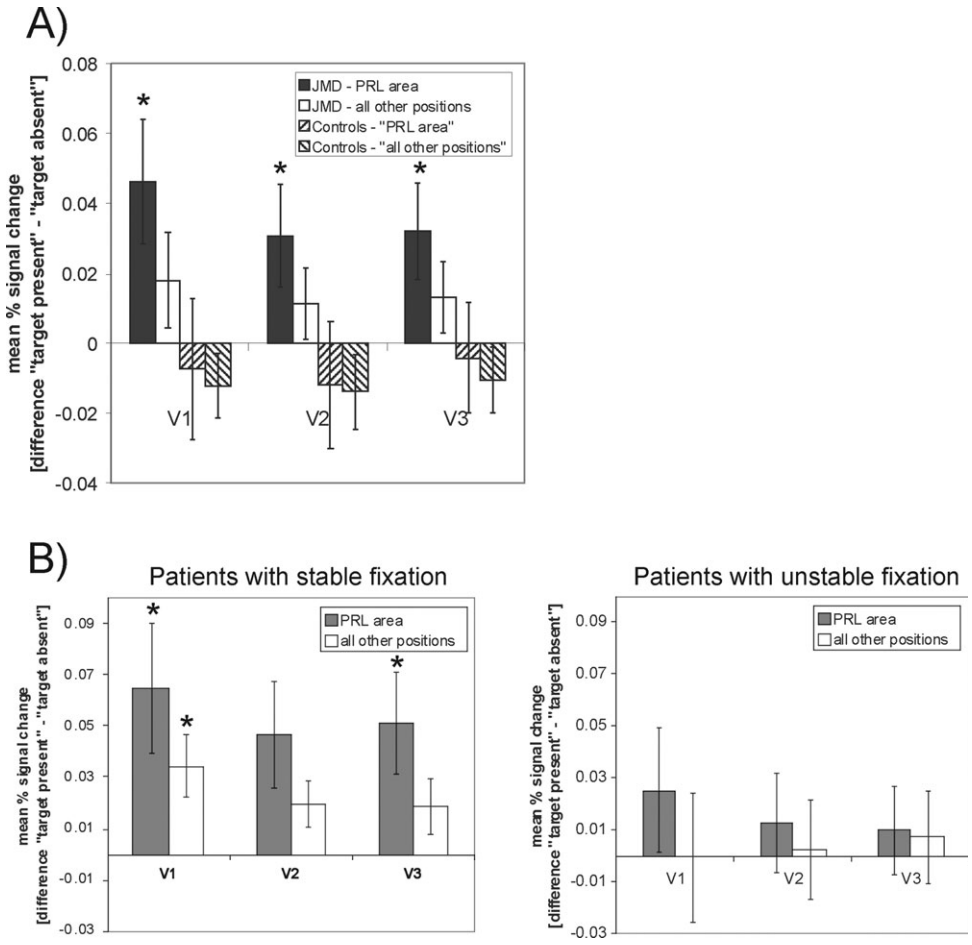

Figure 6.

Mean group differences in percentage BOLD signal change between "target present" vs. "target absent" trials for visual areas V1, V2, and V3, together with their respective standard errors. **A**: Mean group differences for the entire patient group and the control group are shown, separately for the targets in the PRL zone and target at all other positions outside the PRL zone (black and white columns for the patient group, striped columns for the control group. **B**: Mean group differences for the patient sample alone, separated in the group with stable fixation (left) and the group with unstable fixation (right). Dark gray columns represent percent signal change values for trials where the target appeared in the PRL zone, white columns represent percent signal change values for trials where the target appeared at any other position outside the PRL zone. Marked with stars (*) are those columns, which differed significantly ($P \leq 0.05$) from zero.

Thus the mean percent signal change values plotted in Figure 6 all show additional activation on trials where a target was present at the respective positions in the visual field in comparison to nontarget trials. In accordance with the statistical results presented above, this difference is neither significantly different from zero for the control group (Fig. 6A) nor for the patient group with unstable fixation (Fig. 6B right). Figure 6B shows the mean difference in percent signal change for V1, V2, and V3 for the condition, where the target appeared in the PRL zone (gray columns), and the condition, where the target appeared at any other position outside the PRL projection zone (white columns), separately for the group with stable fixation (left) and with unstable fixation (right). Patients with stable fixation exhibit significantly enhanced BOLD percent signal differences on trials where the target fell within the PRL area. Stars mark those mean differences in percent signal change that differed significantly from zero ($P \leq 0.05$). The same holds again for ANOVAs conducted under consideration of an equal number of positions pooled for the "PRL area" (six positions) and the "opposite hemifield" (six positions). In the group with stable fixation this analysis revealed a significant effect of "target present vs. target absent" trials [$F(1,8) = 8.97$; $P = 0.017$] and a significant main effect of "target position" [$F(1,8) = 6.9$; $P = 0.031$]. The main effect "visual area" as well as all

interactions were again not statistically significant (all $P > .05$). In the group with unstable fixation all main effects and interactions yielded no significant results.

DISCUSSION

In this study we examined performance and related brain activity in patients with central visual loss due to hereditary retinal dystrophies while they performed a visual search task in the peripheral visual field. We were interested in the advantage that a stable eccentric fixation can offer to the patients in such a task and whether we could find evidence for an up-regulation in the PRL projection zone. Target stimuli were presented randomly over trials in all parts of the peripheral visual field. Patients with a stable PRL were able to detect target stimuli better than patients with unstable eccentric fixation, not only around their PRL, but also in other parts of the peripheral visual field (Fig. 3). This result appears to be independent of scotoma size, since the scotoma size did not differ significantly between the two patient groups with stable and unstable fixation. Although overall the patients showed lower performance than the controls, the performance level of patients with stable eccentric fixation did not differ significantly from the controls' performance level, when the targets fell in the area of their PRL. False alarm rates were comparably low in both patients and control groups, suggesting that the sensitivity index d' gives reliable values for search performance. An additional analysis of relative frequencies of performance levels across the patient and control groups (Fig. 4) showed that about half of the patients with stable fixation performed better or at least as well as one half of the controls, while patients with unstable fixation overall performed clearly worse. These findings are in line with several studies that showed in the past how patients with central visual field scotomata benefit from training to develop an eccentric fixation, where the improvement in reading speed was usually accompanied by a stabilization of eccentric fixation [e.g. Crossland et al., 2004; Nilsson et al., 1998, 2003; Sunness et al., 1996; Rubin and Feely, 2009; Trauzettel-Klosinski and Tornow, 1996]. Recently Ishiko et al. [2010] also showed a "paradoxical" improvement in visual acuity for the worse eye in patients with age-related maculopathy. While the better eye was deteriorating, this effect could in part be attributed to a more stable eccentric fixation with the worse eye. In our paradigm, unstable fixation could have had the effect that the targets did not always appear at exactly the intended location in the visual field. But since the task was only to make a decision about the "presence" or "absence" of a target at any given trial, the exact position of the target was not relevant for the task and should therefore not have had an effect on overall performance.

We additionally show that performance in the visual search task improved when the target appeared in or near the PRL. This improvement was correlated with a significantly higher BOLD response in early retinotopic areas V1, V2, and V3 during target-present trials. This effect was absent in controls and was more pronounced in the patient group with stable eccentric fixation (Fig. 6).

Different explanations could account for these results. One possibility is that patients chose their PRL according to an intrinsically greater sensitivity at this retinal region that would account for the performance pattern we found here, without a learning process at the PRL being involved. We would argue against this possibility, because in this case fixation stability should not affect performance in the way it did. Additionally controls showed no position dependent differences in performance except for two positions in the upper and lower visual field. This suggests that there is no inherit difference in sensitivity for the selected PRL locations in the healthy retina of the left, right, and lower visual field as such as chosen by the patients in our sample.

Instead we would argue that the performance pattern and enhanced BOLD responses we found in patients are a result of a learning process triggered by the consistent use of their PRL for visual tasks like reading over several years. On the basis of our results we are not able to completely clear up the nature of this learning process, so further studies would be required.

One possibility is that the higher BOLD response in early visual cortex is a manifestation of a form of perceptual learning that, as we hypothesized, has taken place in the PRL projection zone of early visual cortex. In our paradigm participants had to discriminate between the letters "L" and "T" in their peripheral visual field, a task normal sighted controls are able to do, but not necessarily are used to doing so, since they have their fovea for reading. Patients with central vision loss on the other hand rely on their PRL for reading and are thus trained to discriminate letters that appear in that area of their peripheral visual field. Studies have shown that perceptual learning effects are location or stimulus specific and accompanied by increasing BOLD responses in early visual cortex [e.g., Schoups et al., 2001; Schwartz et al., 2002; Sigman et al., 2005; Yotsumoto et al., 2008]. In patients with central vision loss it could be argued that stable eccentric fixation appears to facilitate such perceptual learning processes, as suggested by better performance and the more pronounced BOLD responses in these patients. It should be critically noted that also the patient group with stable fixation did not perform significantly better than the controls, as such enhanced performance could have been regarded as robust evidence for perceptual learning effects. On the other hand, the direct comparison between the performance of the patients and controls at a given eccentric locus might not be fair since a substantial part of our patient sample had rather large scotomata (i.e., seven patients with a scotoma $>15^\circ$ visual angle in diameter) and the disease process could also affect vision at the rim of the scotoma.

An alternative explanation for our results would be that attention triggered the higher BOLD signal in patients in comparison to controls. This could be the case if patients were more able to shift and maintain attention to the peripheral visual field compared with the controls. Attention can modulate neural activity in early visual cortex as was for example shown by Tootell et al. [1998]. As JMD patients learn early in life to use eccentric fixation, their focus of attention might be shifted to the PRL location as a result of such a learning process, which, in line with our results, would enhance visual responses to eccentric stimuli. The observation that these responses are enhanced by task-relevant targets (Fig. 6) further suggests a top-down modulation of cortical response in line with earlier studies [Masuda et al., 2008]. The differences in BOLD responses between patients with stable and unstable fixation might then be explained by the assumption that patients with stable fixation have learned to shift and maintain their attention at the eccentric location in a more efficient manner compared to patients with unstable fixation.

Since these effects are supposed to be due to long lasting learning experiences that the patients come with to the experiment, it is not possible to entirely separate effects from a long-term shift of attention to the PRL from effects resulting from perceptual learning with our paradigm.

Cortical Reorganization in the Visual Cortex of Patients With Central Visual Field Loss

There is considerable controversy over the issue whether there are any signs of cortical reorganization in patients with central scotomata. Although some initial studies pointed to BOLD activations in the lesion projection zone [Baker et al, 2005, 2008; Dilks et al., 2009; Schumacher et al., 2008], subsequent studies [Baseler et al., 2009; Masuda et al., 2008] have placed these preliminary findings in doubt. Using retinotopic mapping in fMRI, Baseler et al. [2011] recently reported findings from eight patients with age-related macular degeneration (AMD) and eight patients with Stargardt's disease suggesting a lack of large-scale reorganization in these patients. Shifts in the size and location of population estimates of the receptive field sizes in the lesion projection zone could be mimicked in healthy control subjects by an artificial scotoma [i.e., 50% mask condition in their Fig. 5, s. Baseler et al., 2011] that was applied to the stimuli during retinotopic masking. Our results are in line with these findings but also point to the special role of the PRL in active vision tasks. We have shown that visual performance (Fig. 3) and the corresponding BOLD response on trials where the letter target was presented in or near the PRL (Fig. 6) are enhanced compared with trials on which the target is presented outside of the PRL zone. These results point to a task-dependent up-regulation of activation in the PRL projection zone. Masuda et al. [2008] argue that the BOLD response in the lesion projection zone is only evident when the patients perform an active visual task, indicative of top-down processing. Interestingly, the BOLD response in the PRL projection zone in three patients with hereditary retinal dystrophies [two with Stargardt\s disease, one with cone-rod dystrophy; see their Fig. 4, Masuda et al, 2008] appears to be up-regulated when the patients performed a one-back visual recognition task. Liu et al. [2010] measured four JMD and four AMD patients under passive and active viewing conditions. They also found enhanced activation in the lesion projection zone in the active task in comparison to the passive viewing task. Additionally they found enhanced activation when stimulating the patients' PRL in comparison to another retinal region with matched eccentricity, both in the respective projection zones, not in the lesion projection zone. Taken together, these findings and the present results point to a task-dependent response pattern in the PRL projection zone. On the other hand, Dilks et al. [2009] found evidence supporting a use-independent reorganization of visual cortex. In their study they found that the foveal projection zone in visual cortex responded equally to ectopic stimuli presented at the PRL and an isoeccentric non-PRL location. With our paradigm and analysis we cannot thoroughly address the question of cortical reorganization in the form of an activation of the lesion projection zone in visual cortex by peripheral stimulation. We found a modest task-dependent up-regulation in visual areas V1, V2, and V3 that was most pronounced when targets where presented around the PRL. We interpret this as enhanced processing of visual information – in this case related to the well-trained shapes of the capital letters T and L – by the PRL projection zone in the cortex. An activation in the foveal confluence would not be expected in our study, but we did not address this question explicitly. Our findings rather point to the possibility that such an up-regulation in neural activation may be the result of prolonged usage for shape discrimination that modifies neural structures at the PRL projection zone. The modulatory role of eccentric fixation stability in our results may serve as evidence for a possible facilitation of a stable PRL in everyday vision in patients with loss of central vision due to hereditary retinal dystrophies.

CONCLUSIONS

We examined the neural correlates of visual search performance in patients with hereditary retinal dystrophies and central scotomata. Compared to age-matched controls, the patients responded best when the target letter was presented in or near their preferred retinal locus (PRL). The BOLD response at that location in the visual field was relatively increased compared to locations outside of the PRL area. Patients with stable fixation showed the greatest effects. We interpret our results as a consequence of prolonged usage of the PRL for shape discrimination. JMD patients with stable eccentric fixation exhibited higher visual search performance compared to patients with

unstable fixation. These results point to the importance of stable eccentric fixation in compensatory processes in the brain of patients with central visual field loss.

ACKNOWLEDGMENTS

The authors thank Anton Beer for his helpful comments to an earlier version of the manuscript, the Pro Retina Foundation and the City of Regensburg (Senior Citizens' Office) for their assistance in participant recruitment as well as all participants of our study.

REFERENCES

Ahissar M, Hochstein S (1997): Task difficulty and the specificity of perceptual learning. Nature 387:401–406.

Bäckman Ö, Inde K (1979): Low Vision Training. Malmö: Hermods.

Baker CI, Dilks DD, Peli E, Kanwisher N (2008): Reorganization of visual processing in macular degeneration: Replication and clues about the role of foveal loss. Vis Res 48:1910–1919.

Baker CI, Peli E, Knouf N, Kanwisher NG (2005): Reorganization of visual processing in macular degeneration. J Neurosci 25:614–618. doi:10.1523/JNEUROSCI.3476-04.2005.

Baseler HA, Gouws A, Morland AB (2009): The organization of the visual cortex in patients with scotomata resulting from lesions of the central retina. Neuroophthalmology 33:149–157.

Baseler HA, Gouws A, Haak KV, Racey C, Crossland MD, Tufail A, Rubin GS, Cornelissen FW, Morland AB (2011): Large-scale remapping of visual cortex is absent in adult humans with macular degeneration. Nat Neurosci 14:649–655.

Beer AL, Plank T, Greenlee MW (2011): Diffusion tensor imaging shows white matter tracts between human auditory and visual cortex. Exp Brain Res 213:299–308.

Beer AL, Watanabe T, Ni R, Sasaki Y, Andersen GJ (2009): 3D surface perception from motion involves a temporal-parietal network. Eur J Neurosci 30:703–713.

Cox RW, Jesmanowicz A (1999): Real-time 3D image registration for functional MRI. Magn Reson Med 42:1014–1018.

Crossland MD, Culham LE, Kabanarou SA, Rubin GS (2005): Preferred retinal locus development in patients with macular disease. Ophthalmology 112:1579–1585.

Crossland MD, Culham LE, Rubin GS (2004): Fixation stability and reading speed in patients with newly developed macular disease. Ophthalmic Physiol Opt 24:327–333.

Dale AM, Fischl B, Sereno MI (1999): Cortical surface-based analysis. I. Segmentation and surface reconstruction. Neuroimage 9:179–194.

Desikan RS, Segonne F, Fischl B, Quinn BT, Dickerson BC, Blacker D, Buckner RL, Dale AM, Maguire RP, Hyman BT, Albert MS, Killiany RJ (2006): An automated labelling system for subdividing the human cerebral cortex on MRI scans into gyral based regions of interest. Neuroimage 31:968–980.

DeYoe EA, Carman GJ, Bandettini P, Glickman S, Wieser J, Cox R, Miller D, Neitz J (1996): Mapping striate and extrastriate visual areas in human cerebral cortex. Proc Natl Acad Sci USA 93:2382–2386.

Dilks DD, Baker CI, Peli E, Kanwisher N (2009): Reorganization of visual processing in macular degeneration is not specific to the "preferred retinal locus". J Neurosci 29:2768–2773.

Fahle M, Poggio T (2002): Perceptual Learning. Cambridge, MA: The MIT Press.

Fischl B, Sereno MI, Dale AM (1999a): Cortical surface-based analysis. II. Inflation, flattening, and a surface-based coordinate system. Neuroimage 9:195–207.

Fischl B, Sereno MI, Tootell RB, Dale AM (1999b): High-resolution intersubject averaging and a coordinate system for the cortical surface. Hum Brain Mapp 8:272–284.

Fischl B, Dale AM (2000): Measuring the thickness of the human cerebral cortex from magnetic resonance images. Proc Natl Acad Sci USA 97:11050–11055.

Fischl B, Liu A, Dale AM (2001): Automated manifold surgery: Constructing geometrically accurate and topologically correct models of the human cerebral cortex. IEEE Trans Med Imaging 20:70–80.

Fischl B, Salat DH, Busa E, Albert M, Dieterich M, Haselgrove C, van der Kouwe A, Killiany R, Kennedy D, Klaveness S, Montillo A, Makris N, Rosen B, Dale AM (2002): Whole brain segmentation: Automated labeling of neuroanatomical structures in the human brain. Neuron 33:341–355.

Fischl B, Salat DH, van der Kouwe, AJ, Makris N, Segonne F, Quinn BT, Dale AM (2004a): Sequence-independent segmentation of magnetic resonance images. Neuroimage 23(Suppl 1):S69–S84.

Fischl B, van der Kouwe A, Destrieux C, Halgren E, Segonne F, Salat DH, Busa E, Seidman LJ, Goldstein J, Kennedy D, Caviness V, Makris N, Rosen B, Dale AM (2004b): Automatically parcellating the human cerebral cortex. Cereb Cortex 14:11–22.

Fletcher DC, Schuchard RA (1997): Preferred retinal loci relationship to macular scotomas in a low-vision population. Ophthalmology 104:632–638.

Furmanski CS.Schluppeck D, Engel SA (2004): Learning strengthens the response of primary visual cortex to simple patterns. Curr Biol 14:573–578.

Gilbert CD, Sigman M, Crist RE (2001): The neural basis of perceptual earning. Neuron 31:681–697.

Guez JE, Le Gargasson JF, Rigaudiere F, O'Regan JK (1993): Is there a systematic location for the pseudo-fovea in patients with central scotoma? Vision Res 33:1271–1279.

Ishiko S, van de Velde F, Yoshida A (2010): Paradoxical improvement of visual acuity in macular disease. Curr Eye Res 35:6451–656.

Kadlec H (1999): Statistical properties of d′ and β estimates of signal detection theory. Psychol Methods 4:22–43.

Karni A, Sagi D (1991): Where practice makes perfect in texture discrimination: Evidence for primary visual cortex plasticity. Proc Natl Acad Sci USA 88:4966–4970.

Kimmig H, Greenlee MW, Huethe F, Mergner T (1999): MR-Eyetracker: A new method for eye movement recording in functional magnetic resonance imaging. Exp Brain Res 126:443–449.

Liu T, Cheung S-H, Schuchard RA, Glielmi CB, Hu X, He S, Legge GE (2010): Incomplete cortical reorganization in macular degeneration. Invest Ophthalmol Vis Sci doi: 10.1167/iovs.09-4926.

Masuda Y, Dumoulin SO, Nakadomari S, Wandell BA (2008): V1 projection zone signals in human macular degeneration depend on task, not stimulus. Cereb Cortex 18:2483–2493.

Nilsson UL, Frennesson C, Nilsson SEG (1998): Location and stability of a newly established eccentric retinal locus suitable for reading, achieved through training of patients with a dense central scotoma. Optom Vis Sci 75:873–878.

Nilsson UL, Frennesson C, Nilsson SEG (2003): Patients with AMD and a large absolute central scotoma can be trained

successfully to use eccentric viewing, as demonstrated in a scanning laser ophthalmoscope. Vis Res 43:1777–1787.

Plank T, Frolo J, Brandl-Rühle S, Renner AB, Hufendiek K, Helbig H, Greenlee MW (2011): Gray matter alterations in visual cortex of patients with loss of central vision due to hereditary retinal dystrophies. Neuroimage 56:1556–1565.

Rubin GS, Feely M (2009): The role of eye movements during reading in patients with age-related macular degeneration (AMD). Neuroophthalmology 33:120–126.

Schoups AA, Vogels R, Orban GA (1995): Human perceptual learning in identifying the oblique orientation: Retinotopy, orientation specificity and monocularity. J Physiol 483:797–810.

Schoups A, Vogels R, Qian N, Orban G (2001): Practising orientation identification improves orientation coding in V1 neurons. Nature 412:549–553.

Schumacher EH, Jacko JA, Primo SA, Main KL, Moloney KP, Kinzel EN, Ginn J (2008): Reorganization of visual processing is related to eccentric viewing in patients with macular degeneration. Restor Neurol Neurosci 26:391–402.

Schwartz S, Maquet P, Frith C (2002): Neural correlates of perceptual learning: A functional MRI study of visual texture discrimination. Proc Natl Acad Sci USA 99:17137–17142.

Segonne F, Dale AM, Busa E, Glessner M, Salat D, Hahn HK, Fischl B (2004): A hybrid approach to the skull stripping problem in MRI. Neuroimage 22:1060–1075.

Segonne F, Pacheco J, Fischl B (2007): Geometrically accurate topology correction of cortical surfaces using nonseparating loops. IEEE Trans Med Imaging 26:518–529.

Sigman M, Pan H, Yang Y, Stern E, Silbersweig D, Gilbert CD (2005): Top-down reorganization of activity in the visual pathway after learning a shape identification task. Neuron 46:823–835.

Sled JG, Zijdenbos AP, Evans AC (1998): A nonparametric method for automatic correction of intensity nonuniformity in MRI data. IEEE Trans Med Imaging 17:87–97.

Sunness JS, Applegate CA, Haselwood D, Rubin GS (1996): Fixation patterns and reading rates in eyes with central scotomas from advanced atrophic age-related macular degeneration and Stargardt disease. Ophthalmology 103:1458–1466.

Timberlake GT, Peli E, Essock EA, Augliere RA (1987): Reading with a macular scotoma. II. Retinal locus for scanning text. Invest Ophthalmol Vis Sci 28(8):1268–1274.

Tootell RBH, Hadjikhani N, Hall EK, Marrett S, Vanduffel W, Vaughan JT, Dale AM (1998): The retinotopy of visual spatial attention. Neuron 21:1409–1422.

Trauzettel-Klosinski S, Tornow RP (1996): Fixation behaviour and reading ability in macular scotoma. Neuroophthalmology 16:241–253.

Watanabe T, Nanez JE, Sasaki Y (2001): Perceptual learning without perception. Nature 413:844–848.

Whittaker SG, Budd J, Cummings RW (1988): Eccentric fixation with macular scotoma. Invest Ophthalmol Vis Sci 29:268–278.

Wickens T (2002): Elementary Signal Detection Theory. New York: Oxford University Press.

Yotsumoto Y, Watanabe T, Sasaki Y (2008): Different dynamics of performance and brain activation in the time course of perceptual learning. Neuron 57:827–833.